Mater. Sci. Eng. A., Vol. 627, pp.145-152, (2015) doi: 10.1016/j.msea.2014.12.084

The effect of electropulsing on the interlamellar spacing and mechanical properties of a hot-rolled 0.14 % carbon steel

A. Rahnama
Department of Materials, Imperial College London
Exhibition road, London, SW7 2AZ, England
R.S. Qin,
Department of Materials, Imperial College London
Exhibition road, London, SW7 2AZ, England

April 27, 2015

Abstract

The application of electropulsing treatment to a low carbon ferritic-pearlitic steel is studied. The effect of electric current pulses on the interlamellar spacing of pearlite is investigated. It is found that the interlamellar spacing increases as the number of pulses increases. The mechanism of electropulse-effect was discussed by analysing the change in the free energy and the reduction of electrical resistance due to electropulsing. Mechanical properties are also examined for the samples with and without electropulsing treatment. It is shown that softening occurs during the treatment which is attributed to the formation of precipitation free zone (PFZ), increase in the value of interlamellar spacing and the spheroidization of the lamellar structure.

Keywords: Electropulsing treatment, phase transformation, diffusion, interlamellar spacing, mechanical properties.

1 introduction

It is known that the electropulsing treatment has characteristics such as fast heating, composite electromagnetic force, reduced thermokinetics potential barrier, and high-speed electron impact. It has been reported that the application of electropulsing could affect precipitation behaviour of precipitated phase in solid state metal [1], thermodynamics and dynamical condition of carbide precipitation [2], the microstructure evolution of solid state metallic materials [3, 4], the strength of the diffusing capacity of carbon atom [5], the nucleation potential barrier and nucleation rate of graphite [6]. It

has been also reported that electropulsing has the capacity to induce new phase and new microstructure formations [7], and to remove inclusions in molten steel [8]. It is believed that the application of electropulsing accelerates solid-state phase transformations in many systems. It has been reported that electropulsing could cause a dramatic increase in diffusion coefficient in Cu-Zn alloys [9]. Furthermore, in highly deformed pearlitic steel, Samuel et al. [10] have reported that high intensity electropulsing introduces changes into microstructure and hardness values and enhances the diffusion coefficient. However, the effect of electropulsing treatment on the interlamellar spacing has not been previously reported in the literature.

In the two-phase ferritic-pearlitic steels, the pearlite phase controls the strength whereas the ferrite governs the ductility [11, 12, 13, 14, 15]. It has been found that microstructural characteristics such as interlamellar spacing along with grain size of the ferrite affect the flow stress of ferritic-pearlitic steels [15]. Moreover, it has been frequently reported that the strength of the pearlite phase follow a linear relationship with respect to the interlamellar spacing [16, 17, 18, 19].

The aim of the present work is to examine the effect of electropulsing on the interlamellar spacing. The treatment was performed at the room temperature and it is found that the interlamellar spacing increases with the number of passing pulses. Electropulsing is able to profoundly affect the lamellar structure even at room temperature with the least energy consumption comparing to other heat treatments.

Mechanical testing are conducted to investigate the effect of the current pulses on the hardness, yield strength, UTS, and elongation.The correlation between hardness or yield strength and interlamellar spacing is studied. Such a research has not been preceded before and therefore could provide a new insight into the electropulsing treatment.

2 Experiment

2.1 Material and Electropulsing

The steel used in this work had a composition (in wt%) of 0.14 C-1.0 Si- 2.1 Mn-0.03 Al-0.025 Nb. The steel was rolled at $800^{\circ}C$ to a sheet with 2.64 mm thickness and then chilled slowly in furnace. The microstructure at ambient temperature was coarse-grained ($> 1\mu m$) ferrite and little cementite. Flat samples were cut as 2-mm long, 3.5-mm wide, and 2.64-mm thick in the middle section of the samples; the length of the two ends of samples was much longer than that of middle part (each was about 14-mm) and the two ends were completely covered by copper electrodes during the electropulsing treatment. Electropulsing was performed under ambient conditions by an Avtech AV-108F-B-P Current Pulser which converts the direct current into pulsed current. The setting is shown in Fig. 1. The direct current power source has standard output power of 80 watts and standard output electric potential of 20 volts. The pulse width, peak current intensity, pulse frequency and pulse trigger mode are programmable. The testing sample was connected with two copper electrodes from both ends to form a current circuit. No internal stress might occur if there was a current-induced temperature rising because both sample and electrodes were hold freely rather

than fixed to certain positions. The waveform of electropulsing was detected in situ by a digital storage oscilloscope TDS3012. All the pulses applied in this work were chosen to have $20\mu s$ pulse width and $1.018 \times 10^7 A/m^2$ peak current density. Three different samples were electropulsed at these conditions each of which with a different number of pulses, namely 20, 100 and 1000 pulses. The temperature was measured by a K-type thermocouple (diameter, 0.08 mm) attached to a sample at its middle most section. The temperature rise due to electropulsing was less than $5°C$ and thus is negligible.

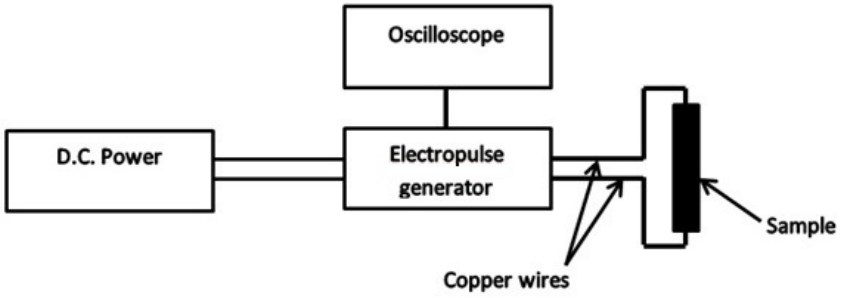

Figure 1: Connection arrangement for the electropulsing treatment.

2.2 Microstructure characterisation

The microstructure of the samples before and after electropulsing treatment were characterised by a LEO Gemini 1525 high resolution field emission gun scanning electron microscope (FEGSEM) operated at 5kV. The equipment was fitted with Oxford instruments INCA energy dispersive and wavelength dispersive x-ray spectrometers. The samples for scattering electron microscopy (SEM) observations were prepared by the conventional method using diamond pastes and etched in 2% nital etching solution. The volume fraction of phases determined using point counting technique and was measured to be 84.5%. It was done through 30 randomly selected fields at a magnification of $\times$100 in the optical microscope. The interlamellar spacing was measured using FE-SEM technique as described in Ref.[20]. On average, 50 pearlite colonies in each sample were characterized for calculating the interlamellar spacing using this technique..

2.3 Mechanical properties

The Vickers hardness was measured using a Zwick digital 3103 IRHD Micro Compact Hardness Tester employing 10-kg load for a dwell time of 10 s. Tensile testing was carried out using Zwick/Roell tensile testing machine at strain rate of $10^{-3}/s$. The machine was fitted with testing software testXpert II. Yield stress (0.2% proof stress), UTS and percent elongation were directly recorded from the results displayed by the computer.

3 Results

3.1 Material and Microstructure

The microstructural characterisation of the steel samples, unelectropulsed and electropulsed with different number of pulses, showed the presence of ferrite and pearlite phases. Fig.2 shows the typical SEM micrograph of various samples under study and clearly demonstrates the presence of pearlite colonies in the ferrite network. The volume fraction of ferrite during the experiment was constant and measured to be 84.5%, and the rest of the volume is occupied by pearlite. The variation of interlamellar spacing with number of electric current pulses is plotted in Fig. 3. The interlamellar spacing was found to increase with increasing the number of pulses as shown in Fig. 4.

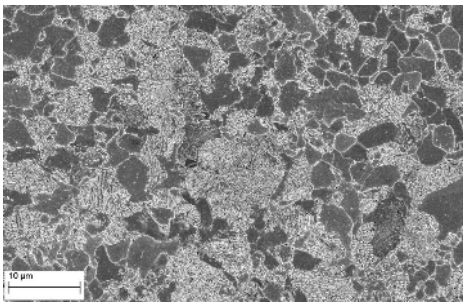

(a)

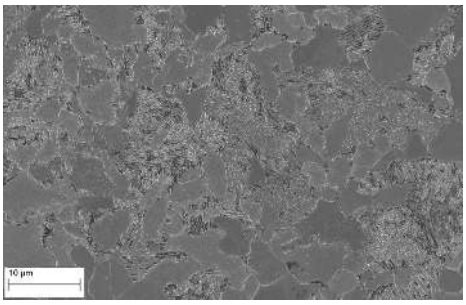

(b)

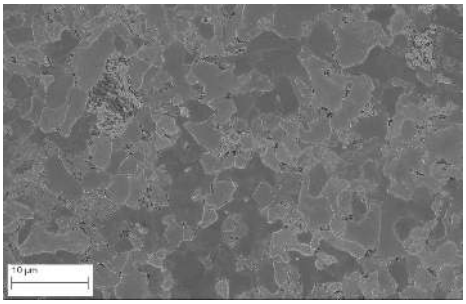

(c)

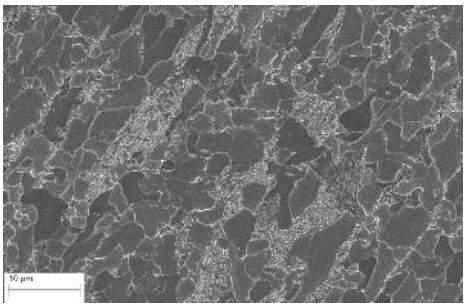

(d)

Figure 2: SEM micrograph of samples (a) before EP, (b) after 20 pulses, (c) after 100 pulses, (d) after 1000 pulses.

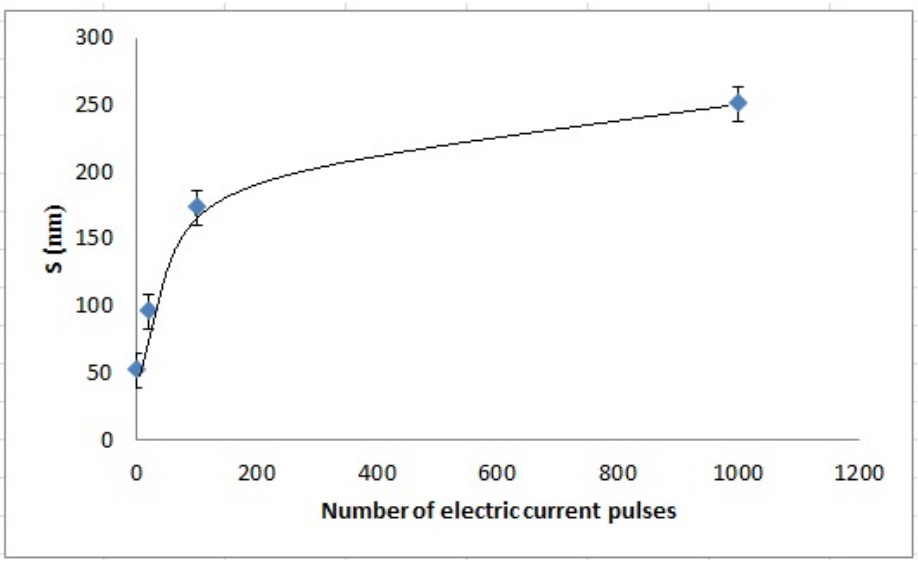

Figure 3: The effect of electropulsing treatment on the interlamellar spacing (S) of the pearlite colonies.

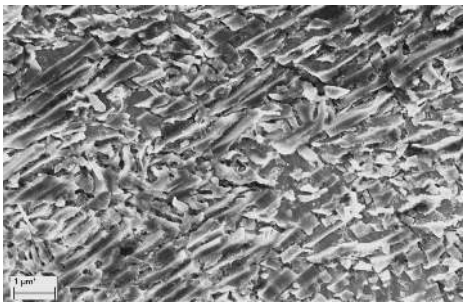

(a)

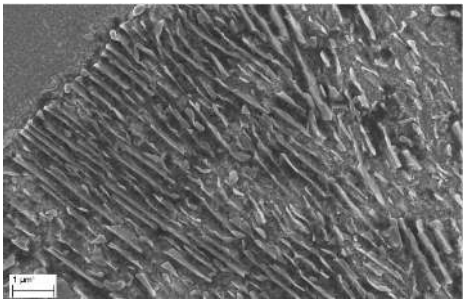

(b)

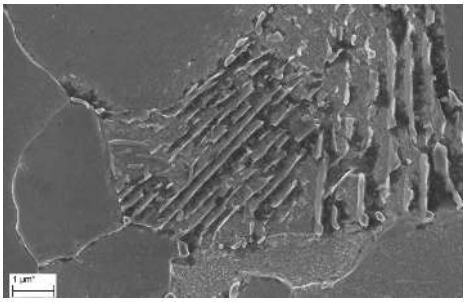

(c)

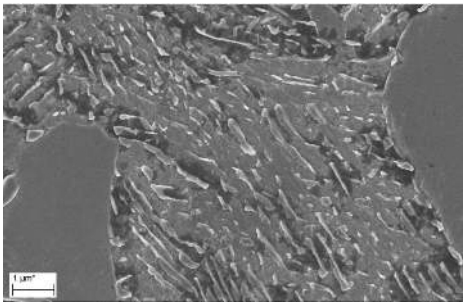

(d)

Figure 4: Lamellar structure for the samples (a) before electropulsing (b) after 20 pulses (c) after 100 pulses and (d) after 1000 pulses.

Electropulsing treatment also resulted in spheroidization of cementite plate. This effect was more apparent at the larger number of pulses as shown in Fig. 5 for the sample with 1000 number of pulses. As can be seen in this figure, fine spheroidal particles distributed within the ferrite matrix.

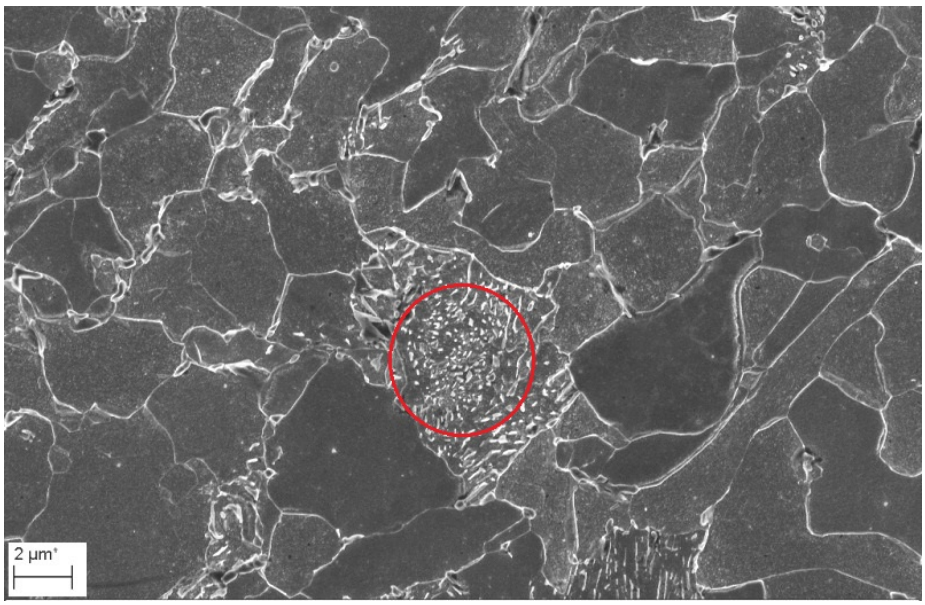

Figure 5: Spheroidization of pearlite due to electropulsing treatment.

3.2 Precipitation free zone (PFZ)

Niobium is one of the elements that forms strong carbide. It is usually used in order to control the austenite grain size during the thermomechanical processing of microalloyed steels. Fig. 6 demonstrates the EDX analysis of the sample treated by 1000 electric pulses. The dark area at grain boundary (spectrum 8) shows that precipitation free zone (PFZ) has been formed after electropulsing, while the adjacent location inside the grain (spectrum 4) indicates that there exists niobium carbide. Such a phenomenon has not been observed in the as-received sample. Other PFZs are indicated by arrows in the micrograph shown in Fig. 6.

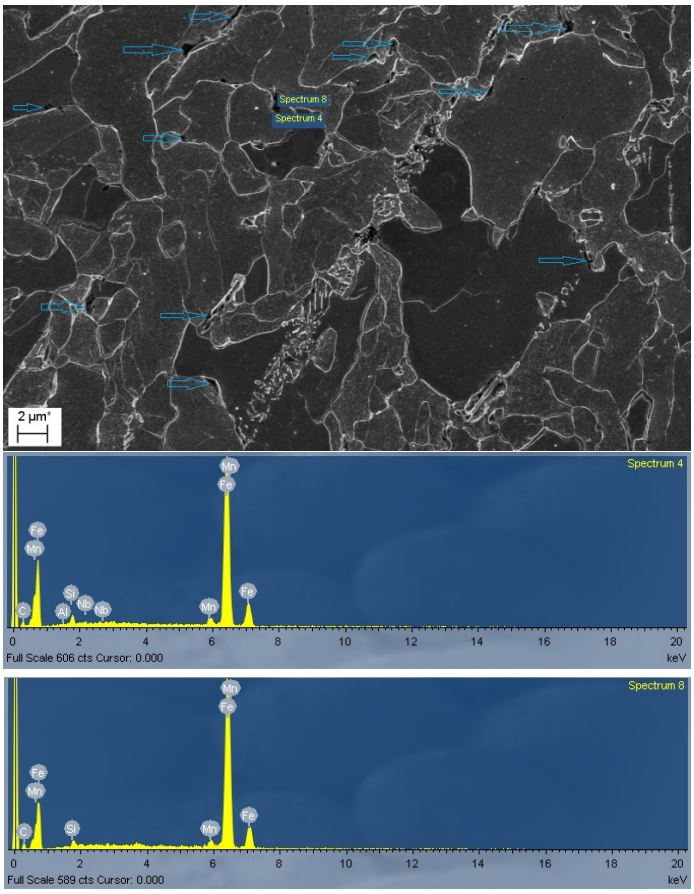

Figure 6: Precipitation free zone formed by electropulsing.

3.3 Mechanical Properties

The stress-strain curves for the samples are presented in Fig. 7. The Vickers hardness and yield strength of the samples are plotted as functions of the number of current pulses and the square root of interlamellar spacing in Fig. 8 and 9, respectively. It is evident from these figures that both harness and yield strength decrease with an increase in the number of electropulses (Fig. 8a and 9a). However, the effect of electropulsing on the values of hardness and yield strength lessens after 100 electric current pulses. It has been frequently reported in the literature [16, 17, 18, 19, 21, 22, 23] that hardness and yield stress follow a Hall-Petch type relationship as follows:

$$H_v = H_0 + K_H S^{-1/2} \tag{1}$$

$$\sigma_y = \sigma_0 + K_y S^{-1/2} \tag{2}$$

where H_v, H_0,σ_y, and σ_0 are the Vickers hardness, the hardness of the ferrite with infinite mean free path, yield strength of the material, and the internal friction strength of the ferrite with infinite mean free path, respectively. K_H and K_y are the dislocation locking constant during hardness measurement and yielding, respectively.

From the plots in Fig. 8b and 9b, intercepts and slopes were calculated and the following empirical relationships were deduced:

$$H_v = 148.36 + 0.6062S^{-1/2} \tag{3}$$

$$\sigma_y = 403.86 + 1.1429S^{-1/2} \tag{4}$$

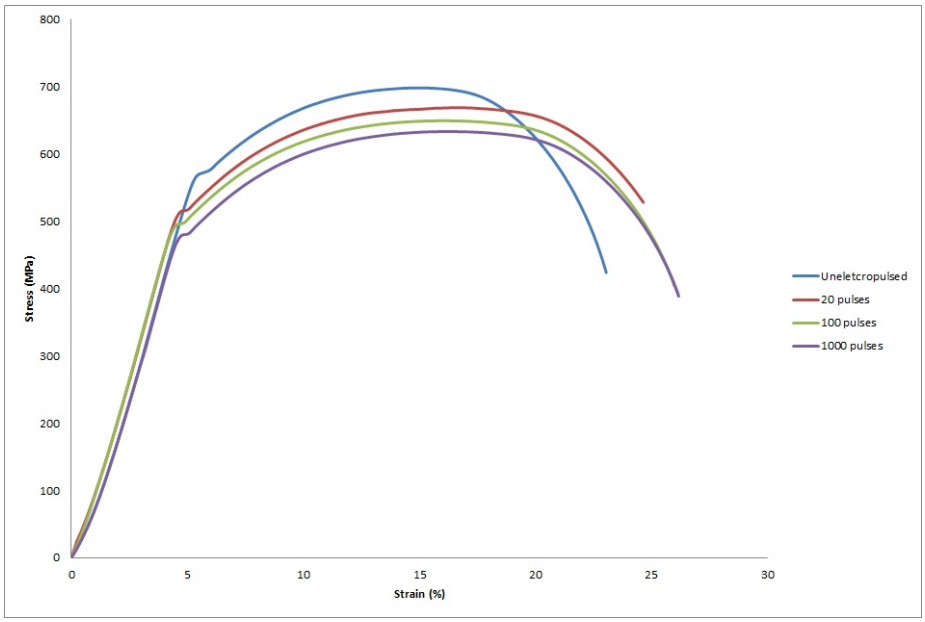

Figure 7: Stress-strain curves for the samples, blue: before electropulsing, red: after 20 pulses, green: after 100 pulses and purple: after 1000 pulses.

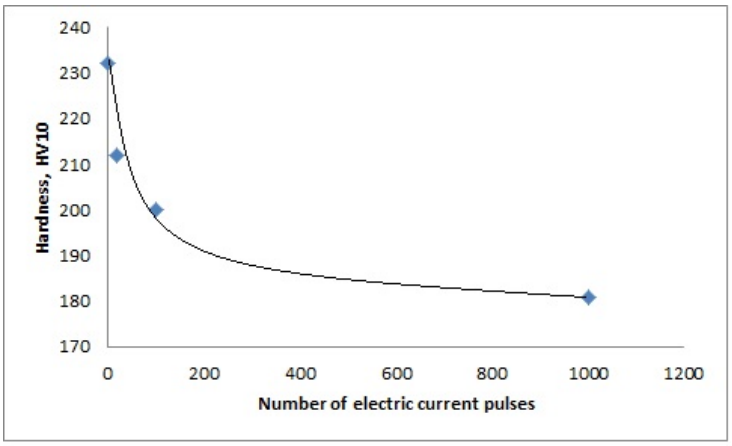

(a)

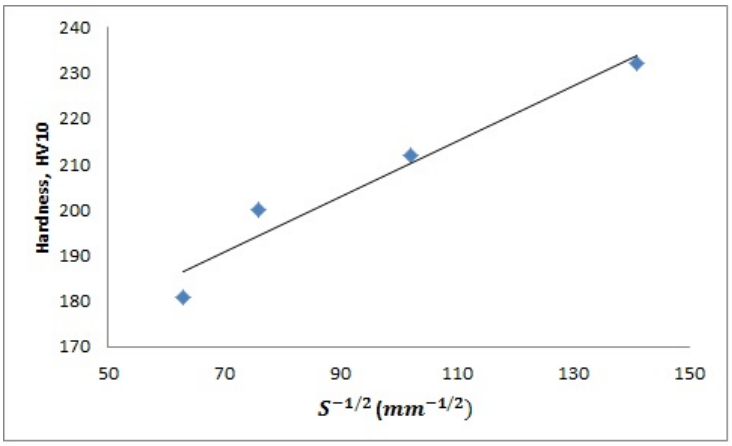

(b)

Figure 8: Graph representing the hardness as a function of (a) the number of electric current pulses and (b) and the square root of the interlamellar spacing of pearlite, *S*.

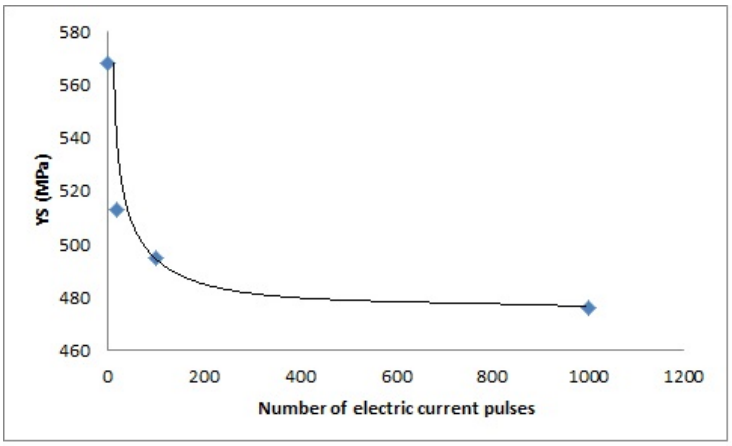

(a)

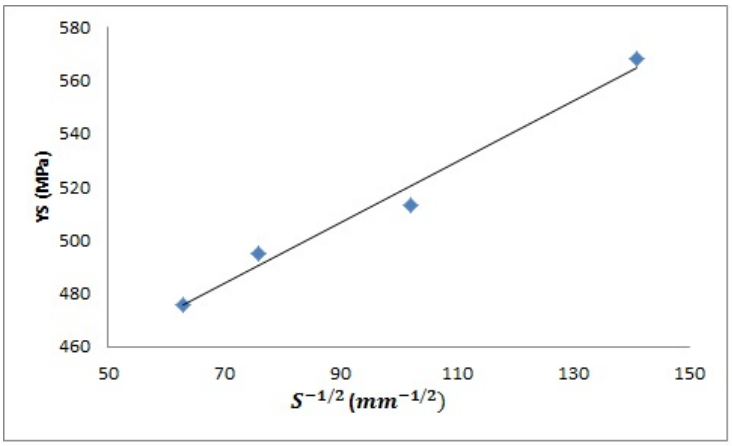

(b)

Figure 9: Graph showing the yield stress as a function of (a) the number of electric current pulses and (b) and the square root of the interlamellar spacing of pearlite, *S*.

Fig. 10a and b show the variation in UTS as functions of the number of electric current pulses and $S^{-1/2}$. UTS plot against the square root of spacing (10a) follows the linear fashion similar to the hardness and yield strength. Fig. 10b shows that the treatment after 100 pulses results in little change in the value of UTS. The following Hall-Petch type of relationship was obtained for UTS:

$$UTS = 582.57 + 0.8187S^{-1/2} \tag{5}$$

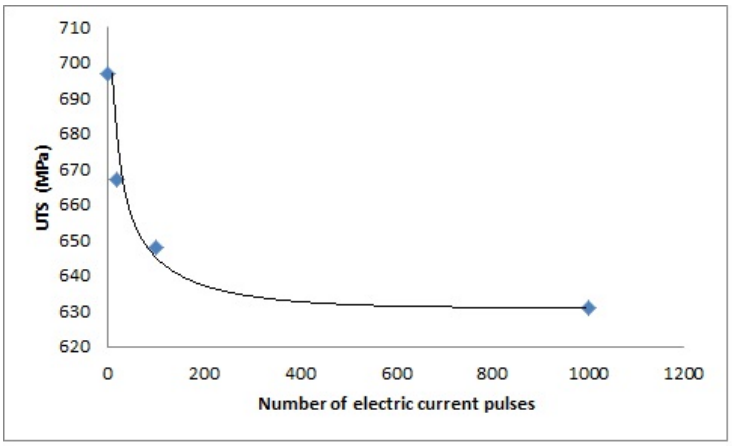

(a)

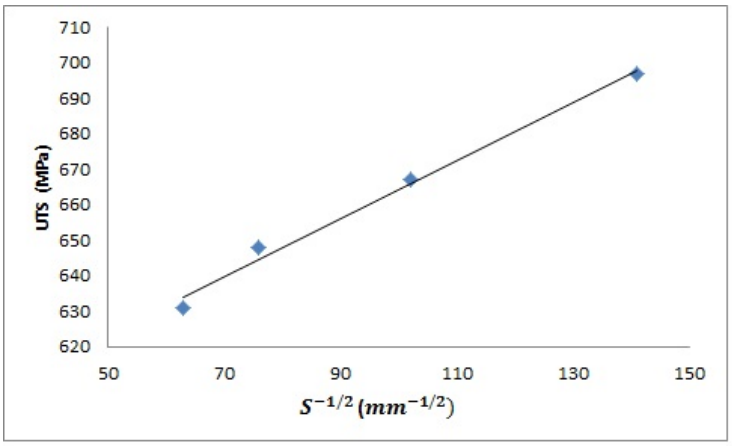

(b)

Figure 10: The variations of the UTS as a function of (a) the number of electric current pulses and (b) the square root of the interlamellar spacing of pearlite, *S*.

Fig. 11a represents the change in percent elongation as a function of the number of current pulses. Electropulsing causes a sharp increase in the value of elongation. However, after 100 pulses, further treatment results in gradual change of the percent elongation. Fig. 11b illustrates the variation of elongation as a function of the square root of interlamellar spacing. The percent elongation decreases with increasing $S^{-1/2}$ in a linear fashion.

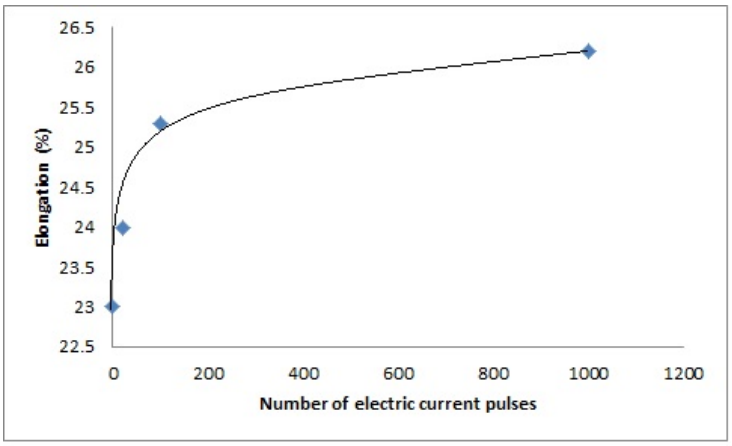

(a)

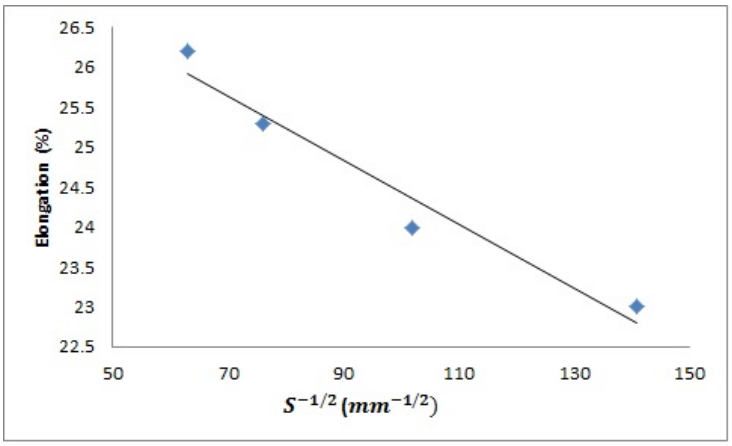

(b)

Figure 11: The changes of the percent elongation as a function of (a) the number of electric current pulses and (b) the square root of the interlamellar spacing of pearlite, *S*.

4 Discussion

4.1 Material and microstructure

4.1.1 Effect of electropulsing on the interlamellar spacing

The steel studied in this investigation consists of pearlite surrounded by the ferrite network. The size of the interlamellar spacing of pearlite was found to increase as the number of electric current pulses was increased. In general, the interlamellar spacing is influenced by the transformation temperature and the interface energy between

ferrite and cementite $\sigma_{\alpha/\theta}$ [24]. The relationships between interlamellar spacing and temperature and interface energy can be express as [25, 26]:

$$S \propto \frac{T_E}{T_E - T} = \frac{1}{1 - \frac{T}{T_E}} \tag{6}$$

and

$$S \propto \sigma_{\alpha/\theta} \tag{7}$$

The increase in the interlamellar spacing of pearlite with the number of pulses can be, then, attributed to a reduction in eutectoid temperature T_E or an increase in interface energy, or both simultaneously. Liu et al.[2] recently reported that electropulsing treatment increases the speed of the precipitation of grain boundary as well as reducing the peak temperature of transformation. In other words, the grain boundary carbides can precipitate at lower transformation temperature, and as a result interlamellar spacing could increase. Another explanation could be presented according to classical thermodynamics as follows: pearlite transformation can be summarized as $\gamma \rightarrow \alpha + Fe_3C$. According to Zener [25], th free energy G, available to form a volume of pearlite of depth δ and interlamellar spacing S growing unidirectionally in the x-direction is:

$$G = \Delta H(\frac{T_E - T}{T_E})S\delta dx\rho \tag{8}$$

where ΔH is the latent heat of transformation. The formation of this new volume of pearlite results in the formation of new ferrite and cementite interfaces and therefore causes an increase in interfacial energy with a value of $2\sigma\delta dx$, where σ is the interfacial energy per unit area. Growth of the lamellae can only takes place if the decrease in energy resulting from the transformation compensates the increase in the interfacial energy [26]:

$$\Delta H(\frac{T_E - T}{T_E})S\rho = 2\sigma \tag{9}$$

The free energy change due to a change in distribution of the current during electropulsing treatment can also be expressed as follows [27]:

$$\Delta G_{EP} = \mu_0 g\xi(\sigma_1, \sigma_2)j^2\Delta V \tag{10}$$

where μ_0 is the magnetic permeability in vacuum, g is a positive geometric factor for coarse grain materials, j is the current density, ΔV is the volume of the phase formed during transformation, and $\xi(\sigma_1, \sigma_2)$ is a factor depending on the electrical properties of the phases and can be defined as [29]:

$$\xi(\sigma_1, \sigma_2) = \frac{\sigma_2 - \sigma_1}{\sigma_1 + 2\sigma_2} \tag{11}$$

where σ_1 and σ_2 are the electrical conductivity of ferrite cementite, respectively. Since the electrical resistivity of cementite is much larger than that of ferrite due to its high carbon and low iron composition, $\xi(\sigma_1, \sigma_2) > 0$. Therefore, $\Delta G_{EP} > 0$

according to Eq. 7. When current pulses are applied, this free energy which is a positive value will be added to the interfacial energy:

$$\Delta H(\frac{T_E - T}{T_E})S\rho = 2\sigma + \Delta G_{EP} \tag{12}$$

As a result, the interlamellar spacing S will increase to compensate the additional energy barrier ΔG_{EP}. The graph of $S^{-1/2}$ as a function of the number of pulses (Fig.9) shows a rapid decrease followed by reaching a certain value (i.e. $S^{-1/2} = 76\ mm^{-1/2}, S = 173\ nm$) after which further treatment results in little change in the value of spacing. Based on the above discussion, we can conclude that energy change due to electropulsing was not enough to cause further increase in the value of interlamellar spacing.

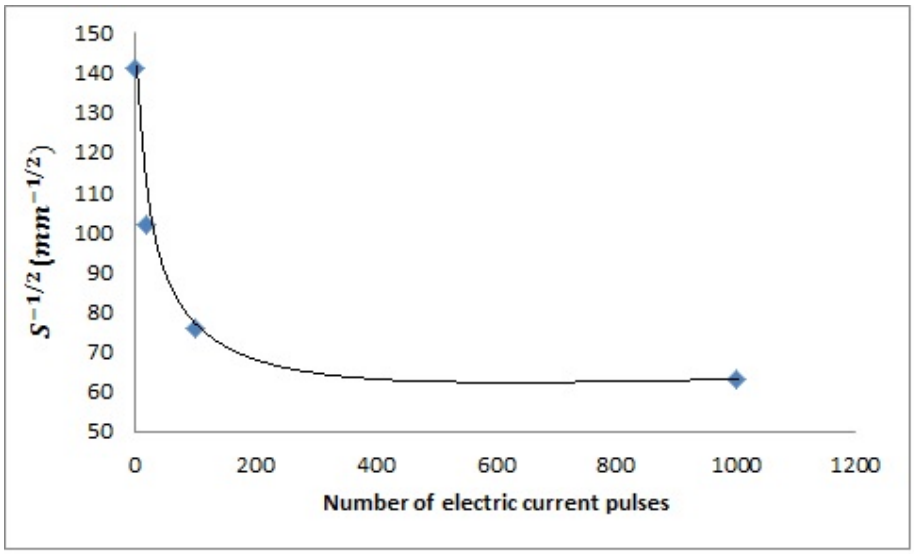

Figure 12: The variation of the root square of the interlamellar of spacing as a function of the number of electric current pulses.

Moreover, thermodynamic calculations show that the electropulsing treatment encourages a structural evolution in materials towards the state with lower electrical resistance [27]. Different types of scattering mechanisms and defects such as morphology of phases, impurities, dislocations and grain boundaries contribute to the value of electrical resistivity [28]. The steel under study has two phases: cementite with higher electrical resistivity than ferrite. In general, the geometric morphology of the phases and their spatial configurations affect the electrical resistivity of the steel. this effect is schematically represented in Fig.13. Suppose that lamellar structure of cementite to have a electrical resistivity of ρ_C and ferrite matrix to have a electrical resistivity of ρ_F, where $\rho_C > \rho_F$. The fractions of both phases are the same in Fig. 13a-d. The steel before electropulsing has a total resistance of $R_a = \frac{\rho_C L}{S}$, where L is the total length of

the sample ans S is the cross section area. This equation gives a value of the electrical resistance close to the cementite. After electropulsing, Fig. 13b, the total electrical resistance can be approximated as $R_b = \frac{\rho_F L}{S_g ap}$, where S_{gap} is the gap area between the fragmentated plates. Thus, it can be concluded that $R_a > R_b > R_c > R_d$. As it has been mentioned earlier, electropulsing treatment tends to arrange the material structure in such a way that its electrical resistance is lowered. Hence, electropulsing promotes a structural evolution towards a state in which the gap area S_{gap} becomes larger resulting in a configuration as illustrated in Fig. 13d. As a result, the interlamellar spacing increases through electropulsing treatment.

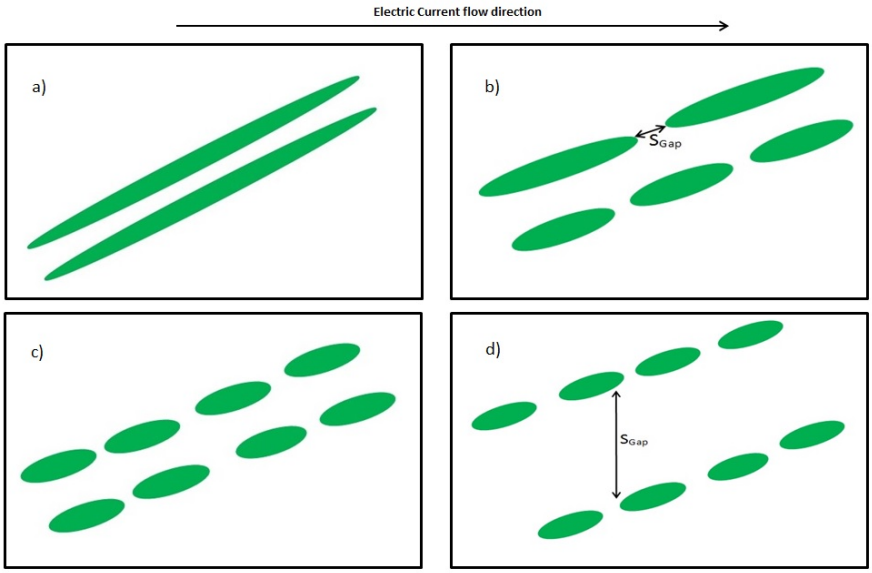

Figure 13: Schematic diagram representing a ferritic-pealitic steel with different phase configurations.

4.1.2 Spheroidization of cementite plates

Macroscopically, the electropulsing treatment is able to configure the conductive phases to a state with maximum percolation effect. In the case of steel under study, the cementite phase has a larger electrical resistivity than ferrite. In addition to cementite high carbon and low iron concentration, the lamellar interconnected cementite plates makes the electrical resistivity of cementite phase large. Fragmentation of the lamellae and formation of discontinuous spherical cementite particles, therefore, allow the formation of more percolation routines within the ferrite matrix. Consequently, Electropulse causes the cementite lamellar to break into small spheres in order to decrease the electric current associated system free energy. Moreover, high dislocation density and high stored energy resulted from rolling provide the high electromigration and enable carbon to diffuse rapidly and help to accomplish the kinetic requirement. According to

Nernst-Einstein equation, the atomic drift flux which takes place with the application of an electric potential to a material can be expressed as [1]:

$$\phi = \frac{ND}{kT} Z^* e \rho j \tag{13}$$

where N is the atomic density, D the pertinent diffusion coeficient, ρ the resistivity and j the current density. Z^* is an effective valence which for carbon atom has been shown to be +4 [30]. It has been found that carbon atoms can electromigrate with the application of a current density of $\sim 10 A cm^{-2}$ which is in good agreement with Eq. 10 [1]. Moreover, vacancies play a key role in precipitation mechanism since they are good nucleation sites for the carbide precipitate [31]. A study of hot deformation of eutetoid plain carbon steel shows that the spheroidisation kinetics was accelerated as much as 10^6 times compared to static annealing [32]. Under electropulsing treatment, the local rapid rise of the temperature generates huge amount of vacancies which are originated from dislocations, interphase and grain boundaries [10]. Ultimately, the generated vacancies electromigrate into grains and causes the enhanced diffusion.

4.1.3 Niobium carbide precipitate

Niobium is usually added to steel in order to control the microstructure and thus to improve the mechanical properties by forming micro- and nano-sized niobium carbide particles. It has been already reported that electropulsing may enhance or retard precipitation processes through various mechanisms [1]. As is evident from Fig. 6, a few PFZs have been formed after treatment. As vacancies act as very good nucleation sites for precipitation, the formation of PFZs can be attributed to the removal of vacancies to sinks such as grain boundaries.

4.2 Effect of electropulsing treatment on mechanical properties

Similar trends were found in all of the mechanical property plots, namely hardness, yield strength, UTS, and elongation. The decrease in these value could be due to various mechanisms such as the formation of PFZs as well as the increase in interlamellar spacing.

The values of these properties show a little change for the number of pulses greater than 100. This is mainly due to the fact that the electropulsing after 100 pulses causes little increase in the value of interlamellar spacing. As it is mentioned earlier the hardness and the yield strength of the steel follow a linear relationship with the root square of interlamellar spacing. In general, the plastic deformation is always associated with the movement of dislocations. When the interlamellar spacing is large, dislocations have enough space to move freely within the matrix. This results in greater deformation and ultimately lower UTS value at larger interlamellar spacing values. The spheroidization of lamellar structure during the treatment also results in the subsequent softening of the structure which in turn reduces the Vickers hardness [10]. The formation of PFZs also plays a key role in weakening the material after electropulsing treatment.

5 Conclusion

Electropulsing treatment was applied to a 0.14 wt.%C steel at room temperature. It is found that interlamellar spacing of pearlite increases with an increase in the number of current pulses applied to the samples. This is attributed to the energy change due to electropulsing which adds to interfacial energy resulting in an increase in the spacing of the lamellar structure. The rate of increase in the interlamellar spacing reduces at certain number of pulses after which further electropulsing results in little change in the spacing of plates. The insufficient energy generated by electropulsing is postulated to be the cause of this phenomenon. Moreover, electropulsing treatment caused spheroidization in the lamellar structure. This results in a substantial softening of the samples. Mechanical testing was carried out for the unelectropulsed sample and the three electropulsed samples. The decrease in the values of mechanical properties can be due to the removal of vacancies and thus forming PFZs along grain boundaries as well as the increase in the value of interlamellar spacing. It is found that the hardness, yield strength and UTS follow a Hall-Petch type of relationship with interlamellar spacing. Finally, electropulsing shows a very promising treatment that can be manipulated to generate various interlamellar spacing without elevating the temperature to austenitization temperature and therefore consumes vary smaller amount of energy comparing with other kinds of heat treatments.

Acknowledgement

The authors wish to acknowledge the financial support from POSCO, TATA and the Royal Academy of Engineering at United Kingdom.

References

References

[1] H. Conrad, Mater. Sci. Eng. A 287 (2000) 227-237.

[2] Y. Liu, L. Wang, H. Liu, B. Zhang, G. Zhao, Trans. Nonfer. Met. Soc. China 21 (2011) 1970-1975.

[3] B. Malard, J. Pilch, P. Sittner, R. Delville, C. Curfs, Acta Mater. 59 (2011) 1542-1556.

[4] A. Rahnama, R. S. Qin, Scripta Mater. 96 (2015) 17-24.

[5] Q. Li, G. Chang, Q. Zhai, 2009. J. Mater. Process. Technol. 209 (2009) 2015-2020.

[6] Y. Peng, Z. Fu, W. Wang, J. Zhang, Y. Wang, Y. Wang, H. Wang, Q. Zhang, 2008. Scr. Mater. 58 (2008) 49-52.

[7] R.S. Qin, E.I. Samuel, A. Bhowmik, J. Mater. Sci. 58 (2011) 49-52.

[8] X.F. Zhang, W.J. Lu, R.S. Qin, Scr. Mater. 69 (2013) 453-456.

[9] Y.Z. Zhou, W. Zhang, J. Guo, G. He, Philos. Mag. Lett. 84 (2004) 341-348.

[10] E.I. Samuel, A. Bhowmik, R.S. Qin, J. Mater. Res. 25 (2010) 1020-1024.

[11] T. Gladman, I.D. Molror, F.B. Pickering, J. Iron Steel Inst. 210 (1972) 916-930.

[12] B. Karlson, G. Linden, Mater. Sci. Eng. 17 (1975) 209-219.

[13] P.H. Chang, A.G. Preban, Acta Metall. 33 (1985) 893-903.

[14] I. Tamura, Y. Tomota, A. Akao, M. Ozawa, S. Kanlani, Trans. Iron Steel Inst. Japan 13 (1973) 283-292.

[15] T. Gladman, F.B. Pickering, In: T.N. Baker (Eds), Yield flow and fracture of polycrystals, Applied Science Publication, London, 1983, 141-198.

[16] O.P. Modi, N. Deshmukh, D.P. Mondal, A.K. Jha, A.H. Yegneswaran, Mater. Charact. 46 (2001) 347-352.

[17] A.R. Marder, B.L. Bramfitt, Metall. Trans. 7A (1976) 365-372.

[18] Hysak J.M., Bernstein I.M. 1976. The role of microstructure on the strength and toughness of fully pearlitic steel. Metallurgical Transactions 7A:1217-1224.

[19] M. Dollar, I.M. Bernstein, A.W. Thompson, Acta Metall. 36 (1988) 311-320.

[20] A.M.Elwazri, P.Wanjara, S.Yue, Mater. Char. 54 (2005) 473.

[21] J.G. Sevillano, In: Gerold V, Kostorz G (Eds). Proceedings of ICSMA-5. Pergamon, Oxford, (1979) pp.819-822.

[22] K.K. Ray, D.P. Mondal, Acta Metall. Mater. 39 (1991) 2201-2206.

[23] L.M. Brown, R.K. Ham, 1971. Strengthening methods in crystals. In: Nicholson RB (Eds), Applied Science PublicationsLondon, (1971), pp.12-25.

[24] J. Li, W. Liu, J. Magn. and Magn. Mater. 362 (2014) 159-164.

[25] C. Zener, Trans. Am. Inst. of Min. and Metall. Eng. 167 (1946) 550-595.

[26] H. K. D. H. Bhadeshia, R. W. K. Honeycombe, Steels microstructure and properties, 3rd ed., Elsevier Ltd, (2006).

[27] Y. Dolinsky, T. Elperin, Phys. Rev. B 47 (1993) 778-785.

[28] F. Khodabakhshi, M. Kazeminezhad, Mater. Des. 32 (2011) 3280-3286.

[29] Y.S. Zheng, G.Y. Tang, J. Kuang, X.P. Zheng, J. Alloy. Compd. 615 (2014) 849-853.

[30] T. Okabe, A.G. Guy, Metall. Trans. 1 (1970) 2705-2713.

[31] H. Conrad, Y. Chen, H.A. Lu, In: P.k. Liaw, R. Viswanathan, K.L. Murty, E. Simonen, D. Frear, (Eds). TMS, Warrendale, PA, (1993) 279.

[32] S. Chattopadhyay, C.M. Sellars, Acta Metall. 30 (1982) 157-170.